ELSEVIER

Journal of Organometallic Chemistry 497 (1995) 149–159

Journal of Organometallic Chemistry

Monitoring the electronic features of rigid C_1-bridged Group 4 ansa-metallocenes by using the dynamic and structural properties of their s-*cis*-η^4-butadiene complexes ☆

Tobias Bürgi [a], Heinz Berke [a,*], Doris Wingbermühle [b], Christian Psiorz [b], Ralf Noe [b], Thomas Fox [b], Markus Knickmeier [b], Martin Berlekamp [b], Roland Fröhlich [b], Gerhard Erker [b,*]

[a] *Anorganisch-chemisches Institut, Universität Zürich, Winterthurerstraße 190, CH-8057 Zürich, Switzerland*
[b] *Organisch-chemisches Institut, Universität Münster, Corrensstraße 40, D-48149 Münster, Germany*

Received 19 January 1995

Abstract

The six-membered ring annulated C_1-bridged ansa-metallocene [(4-cyclopentadienylidene)-4,7,7-trimethyl-4,5,6,7-tetrahydroindenyl]zirconium dichloride (**6a**) was treated with "butadiene-magnesium" to yield the corresponding (s-*cis*-η^4-butadiene)ansa-zirconocene complex as a mixture of two diastereoisomers (**8a**/**8a'**). Their mutual interconversion was monitored by dynamic ^{1}H NMR spectroscopy at high temperatures. The Gibbs activation energy of the thermally induced **8a** ⇌ **8a'** (butadiene)metallocene ring topomerization is $\Delta G^{\neq}_{inv}$ (368 K) = 20.2 ± 0.5 kcal mol^{-1}. This is about 8 kcal mol^{-1} higher than observed for the analogous (σ^2,π-butadiene)metallocene ring inversion process in the parent bis(cyclopentadienyl)zirconium system. The corresponding (s-*cis*-η^4-butadiene)ansa-hafnocene complex (**9**/**9'**) was prepared analogously. Its (η^4-butadiene)Hf inversion barrier ($\Delta G^{\neq}_{inv}$ (268 K) = 14.9 ± 0.5 kcal mol^{-1}) is about 7 kcal mol^{-1} higher than that of the (s-*cis*-η^4-butadiene)$HfCp_2$ reference. The (s-*cis*-η^4-butadiene)[7-*n*-butyl-(4-cyclopentadienylidene)4,7-dimethyl-4,5,6,7-tetrahydroindenyl]zirconium complex **8b** was characterized by X-ray diffraction. The η-butadiene ligand exhibits only a small C–C bond alternation (1.38(2), 1.36(2) and 1.40(2) Å) and a relatively small difference of the butadiene $C_{terminal}$–Zr (2.324(12) and 2.301(13) Å) vs. $C_{internal}$–Zr (2.445(13) and 2.422(13) Å) bond lengths. This points to an increased π complex character of the rigid ansa-metallocene complex compared with the parent (s-*cis*-η^4-butadiene)zirconocene complex **2a** whose structure was determined as a reference (**2a**: butadiene $C_{terminal}$–Zr, 2.332(5) and 2.302(5) Å; $C_{internal}$–Zr, 2.491(6) and 2.480(5) Å). A theoretical extended Hückel theory analysis has revealed that the pronounced increase in the butadiene metallocene topomerization barrier on going from the "normal" bent metallocene (D(1)–Zr–D(2), 126.2°, where D(1) and D(2) denote the centroids of the Cp rings) to the strained C_1-bridged ansa-metallocene complex **8** containing a markedly opened bent metallocene wedge (**8b**: D(1)–Zr–D(2), 114.7°) is electronic in origin, probably caused by closing the energy gap between the $2a_1$ and b_1 frontier orbitals. We conclude that the stereoelectronic features of the bent metallocenes can be controlled by the application of specific steric constraints.

Keywords: Ansa-metallocenes; (Butadiene)metallocene complexes; Dynamic behaviour; EHT calculations; Fluxionality

1. Introduction

In two seminal papers, Brintzinger and Bartell [1] and Lauher and Hoffmann [2] described the essential stereoelectronic properties of the bent metallocene complexes nearly two decades ago using molecular orbital theory. Meanwhile Group 4 bent metallocene complexes activated by various means, but especially by the action of excess methylalumoxane, have turned out to be invaluable homogeneous Ziegler-type catalysts for α-olefin coupling [3]. In particular, many variations of the ansa-metallocenes introduced by the Brintzinger group have essentially contributed to the rapid development of Group 4 metallocene-based homogeneous Ziegler-type α-olefin polymerization [4]. The rigid ansa-metallocene framework has allowed the introduction of high stereocontrol, brought about by selective

☆ Dedicated to Professor Hans-H. Brintzinger on the occasion of his 60th birthday.

* Corresponding authors.

SSDI 0022-328X(95)00112-3

steric shielding of sectors by substituents and annulated ring systems [5]; at the same time it has led to very high catalyst activities, a feature that is probably at least in part due to the special electronic situation at the very ansa-metallocene framework [6].

Most Group 4 bent metallocene complexes, including many ansa-metallocenes, exhibit a backbone that is characterized by D(1)–M–D(2) angles of 125° or greater (D(1) and D(2) denote the centroids of the Cp ring systems) [7]. For such a geometric situation the three valence orbitals ($1a_1$, b_2 and $2a_1$; see below) that are available for bonding of incoming ligands are oriented in the Cp–M–Cp bisecting major plane of the molecule and have their largest extensions toward the open front side of the bent metallocene wedge. There is a substantial separation from the next-highest unoccupied orbital (b_1) that is oriented perpendicularly to this plane. This very special molecular orbital situation [1,2] has been responsible for a variety of particular coordination properties of Group 4 bent metallocene complexes, such as the formation of stable mononuclear (s-*trans*-η^4-butadiene)MCp_2 systems (M = Zr or Hf) [8–10]. Also, the (s-*cis*-η^4-butadiene)zirconocenes and (s-*cis*-η^4-butadiene)hafnocenes are special; they show a very high metallacyclopentene character and are best described as (σ^2,π-C_4H_6)metal complexes [11]. Consequently, the activation barrier of their (σ^2,π-butadiene)metallocene envelope inversion process is very low ($\Delta G^{\neq}_{inv}$ = 12.6 kcal mol^{-1} for **2a** (M = Zr) at 253 K, 8.1 kcal mol^{-1} for **3** (M = Hf) at 165 K) [12]:

We have recently described a novel ansa-metallocene system, the [7-alkyl-(4-cyclopentadienylidene)-4,7-dimethyl-4,5,6,7-tetrahydroindenyl]MCl_2 complexes (**6** and **7**) (see Scheme 1) that contain an extremely rigid bent metallocene backbone. The zirconium and hafnium complexes exhibit the lowest D(1)–M–D(2) angles observed so far (about 115°) and the corresponding very active metallocene–methylalumoxane Ziegler-type catalyst shows a variety of uncommon features [13]. It is tempting to speculate that the very low D(1)–M–D(2) angles have led to a substantial narrowing of the $2a_1/b_1$ valence orbital gap in these systems and thus introduced a novel electronic component of controlling the ligand properties at the front side of the bent metallocene wedge. One might expect that the structural and dynamic features of an η^4-coordinated butadiene ligand system would respond very sensitively to such changes in the electronic environment and could therefore be

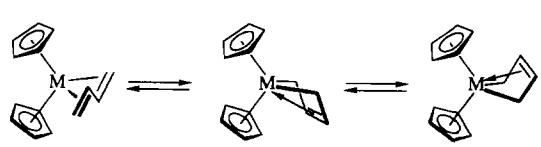

1 **2a** M = Zr, **3** M = Hf

Form 1.

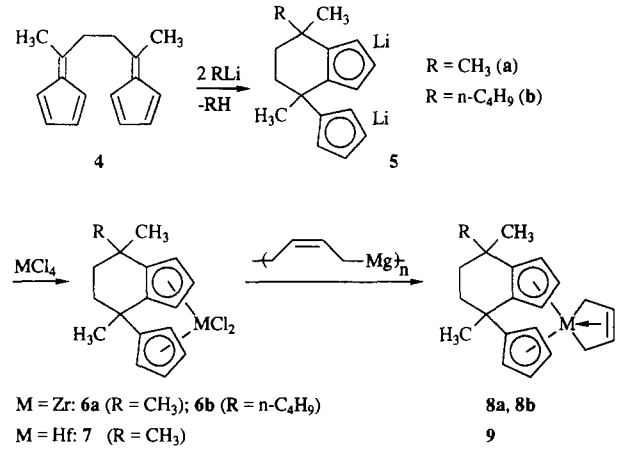

Scheme 1.

suited to monitor even subtle changes in the stereoelectronic characteristics at the bent metallocene framework it is coordinated to. Therefore we have prepared the butadiene complexes of several of our new C_1-bridged ansa Group 4 metallocenes and compared their structural and dynamic features with those of the parent (butadiene)MCp_2 complexes.

2. Results and discussion

2.1. Synthesis of the (butadiene) Group 4 metallocenes and characterization of their dynamic behavior in solution

The fused ligand system of the ansa-metallocenes employed in this study were prepared starting from 2,5-bis(cyclopentadienylidene)hexane (**4**) [13,14]. The bisfulvene was treated with two molar equivalents of methyllithium or *n*-butyllithium respectively to yield the required ligand systems as the dilithio derivatives **5**. Subsequent treatment with zirconium tetrachloride gave the metallocene dihalides **6a** and **6b**; the analogous reaction of **5a** with hafnium tetrachloride furnished the corresponding hafnocene dichloride complex **7** (Scheme 1).

Complex **6a** was treated with one molar equivalent of the oligomeric butadiene dianion equivalent "butadiene-magnesium" [15] in ether–pentane at −78 °C. The mixture was warmed to room temperature and worked up. Crystallization from the ether–pentane solvent mixture yielded the pure (butadiene)metallocene complex **8a**.

Because of the asymmetry of the bent metallocene framework (symmetry group C_1) the possible formation of a total of four diastereomeric (η^4-butadiene)[(4-cyclopentadienylidene)-4,7,7-trimethyl-4,5,6,7-tetrahydroindenyl]zirconium complexes can be envisaged, namely two (s-*trans*-η^4-C_4H_6)metallocene and two (s-

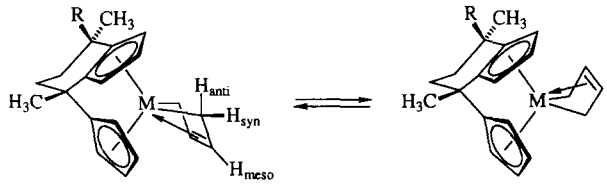

M = Zr, R = CH_3: **8a/8a'** (1.5 : 1); $\Delta G^{\ddagger}_{inv}$(368 K) = 20.2±0.5 kcal mol^{-1}
M = Zr, R = n-C_4H_9: **8b/8b'** (1.5 : 1); $\Delta G^{\ddagger}_{inv}$(368 K) = 20.3±0.5 kcal mol^{-1}
M = Hf, R = CH_3: **9/9'** (1.5 : 1); $\Delta G^{\ddagger}_{inv}$(268 K) = 14.9±0.5 kcal mol^{-1}

Scheme 2.

cis-η^4-C_4H_6)metallocene isomers. In this case, only two of these are formed. They both contain the η^4-coordinated s-*cis*-butadiene ligand. Formation of the isomeric s-*trans* complexes was not observed. Even photolysis under suitable conditions [8] (HPK 125; Pyrex filter; −78 °C; in toluene-d_8; followed by ^{1}H NMR analysis at low temperature) did not lead to the generation of any measurable quantity of the (s-*trans*-conjugated diene)metallocene isomer.

Two (s-*cis*-η^4-butadiene)metallocene complexes **8a** and **8a'** are obtained in a 1.5 : 1 ratio (Scheme 2). This represents the equilibrium ratio at ambient temperature (see below). They can easily be distinguished by their ^{1}H and ^{13}C NMR spectra, although an absolute assignment as to which set of signal represents which particular geometric isomer is not yet possible. The major isomer exhibits seven cyclopentadienyl ^{1}H NMR methine resonances (in *o*-xylene-d_{10}; 600 MHz) at δ = 6.09, 5.54, 5.47, 5.17, 4.73, 4.54 and 4.36 ppm, whereas the corresponding signals of the minor isomer appear at δ = 5.44, 5.32, 5.24, 5.20, 4.70, 4.69 and 4.49 ppm. Each isomer exhibits a complex butadiene ^{1}H NMR pattern involving spin systems of six independent ^{1}H nuclei. The butadiene H_{anti} ^{1}H NMR resonances appear in a typical range at negative δ values (major isomer, δ = −0.84 and −1.07 ppm; minor isomer, δ = −0.91 ppm) (Fig. 1), whereas the H_{syn} proton signals are at δ = 3.55 and 3.43 ppm (major isomer) and δ = 3.4 ppm (minor isomer). The H_{meso} ^{1}H NMR signals of the butadiene ligand in the **8a/8a'** isomer system are observed at around δ = 4.85 ppm. These chemical shift values are quite characteristic of (s-*cis*-η^4-butadiene) Group 4 metallocene complexes. Each of the two (s-*cis*-η^4-butadiene)zirconocene isomers **8a** and **8a'** shows a set of three different methyl groups. Their corresponding ^{1}H NMR resonances are nicely distinguished (δ = 0.96, 1.00 and 1.60 ppm (major isomer); δ = 1.18, 1.39 and 1.57 ppm (minor isomer)).

The (s-*cis*-η^4-butadiene)metallocene isomers **8a** and **8a'** equilibrate by inversion of the M(C_4H_6) envelope structural moiety. This process was monitored by temperature dependent ^{1}H NMR spectroscopy (xylene-d_{10} solvent; 600 MHz) in the temperature range between room temperature and 383 K. The pair of methyl group singlets at δ = 1.60 and 1.57 ppm (1.5 : 1 intensity ratio) turned out to be suited to determine the activation energy of the thermally induced **8a** ⇌ **8a'** interconversion. The analysis of the dynamic NMR spectra was carried out by means of a line shape calculation using the DNMR5 program package [16]. For the **8a** ⇌ **8a'** isomerization a Gibbs activation energy $\Delta G^{\neq}_{inv}$ of 20.2 ± 0.5 kcal mol^{-1} at 368 K was obtained by this procedure [17]. It should be noted that the $\Delta G^{\neq}_{inv}$ barrier of the (s-*cis*-η^4-butadiene)[(4-cyclopentadienylidene)-4,7,7-trimethyl-4,5,6,7-tetrahydroindenyl]zirconium system (**8a/8a'**) is about 8 kcal mol^{-1} higher than was observed for the (s-*cis*-η^4-butadiene)$ZrCp_2$ system **2a** (see above) [11,12]. This enormous increase in the butadiene inversion barrier is characteristic of this particular ansa-metallocene framework and probably reflects an altered electronic situation brought about by enforcing a smaller D(1)–M–D(2) angle (i.e. a wider opening of the bent metallocene wedge).

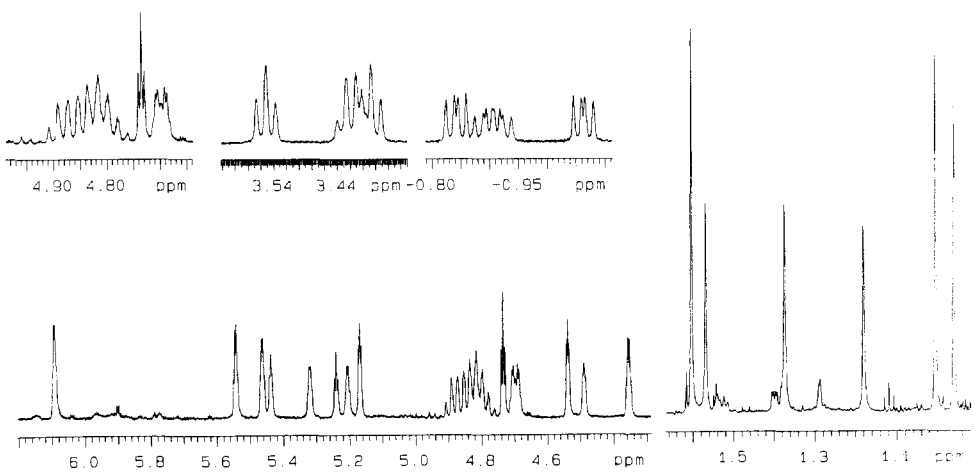

Fig. 1. ^{1}H NMR spectrum (600 MHz) of the **8a–8a'** mixture (in xylene-d_{10} at 300 K).

Table 1
A comparison of selected structural data of (s-*cis*-η^4-conjugated diene)zirconocene complexes

Compound [a]	Zr–C(1)/C(4) (Å)	Zr–C(2)/C(3) (Å)	C(1)–C(2) (Å)	C(2)–C(3) (Å)	C(1)–Zr–C(4) (°)	Zr–C(1)–C(2) (°)	C(1)–C(2)–C(3) (°)	D(1)–Zr–D(2) (°)
2b	2.289(4)	2.714(5)	1.473(4)	1.392(2)	79.3(1)	89.7(4)	121.3(1)	123.4
2c	2.279(2)	2.635(6)	1.465(3)	1.379(4)	82.2(4)	86.6(2)	123.5(2)	125.8
2d	2.300(3)	2.597(3)	1.451(4)	1.398(4)	80.2(1)	84.4(2)	122.7(3)	123.9
2e	2.318(2) [b]	2.574(2)	1.454(3)	1.391(2)	87.3(1)	82.7(2)	128.6(2)	123.2
2f	2.317(3)	2.550(5)	1.445(2)	1.398(3)	88.7(2)	81.8(1)	129.6(3)	124.4
2a	2.316(5) [b]	2.485(6) [b]	1.403(9) [b]	1.365(9)	84.8(3)	79.7(3)	129.6(6)	126.2
8b	2.312(13) [b]	2.444(13) [b]	1.39(2) [b]	1.36(2)	83.3(5)	78.0(8)	126.7(14)	114.7

[a] Data for **2a** and **8b** from this work; data for **2b–2f**, from [12].
[b] Averaged values.

This effect seems to be rather general. It is observed at about the same magnitude also with the other two (butadiene)ansa-metallocene complexes looked at in this study. The reaction of the bisfulvene **4** with *n*-butyllithium furnished a single isomer of the ansa-zirconocene dichloride (**6b**) after purification, namely the isomer with the *n*-butyl group at the position C(7) oriented *cis* to the methyl substituent at C(4). Subsequent reaction of **6b** with the "butadiene-magnesium" reagent again produced only two (s-*cis*-η^4-C_4H_6)ansa-metallocene diastereoisomers, that are formed again in an approximate 1.5 : 1 ratio under conditions of thermodynamic control. Each of the **8b/8b′** isomers again exhibits seven ^{1}H NMR cyclopentadienyl methine resonances and a pair of methyl signals. The ^{1}H NMR methyl singlets at $\delta = 1.61$ ppm (major isomer) and $\delta = 1.58$ ppm (minor isomer) were used to follow the thermally induced **8b** ⇌ **8b′** isomerization by dynamic ^{1}H NMR spectroscopy and to determine the (s-*cis*-η^4-butadiene)ansa-zirconocene inversion barrier. A Gibbs activation energy $\Delta G^{\neq}_{inv}$ (368 K) of 20.3 ± 0.5 kcal mol^{-1} was obtained.

The (butadiene)ansa-hafnocene complex **9** was prepared analogously. Again, only s-*cis*-η^4-butadiene complexes were obtained (**9** and **9′** in a 1.5 : 1 mixture). These hafnium complexes show dynamic ^{1}H NMR behavior because of their mutual rearrangement at much lower temperatures compared with the **8/8′** systems. Again, the $\Delta G^{\neq}_{inv}$ barrier was determined using the methyl group resonance coalescence. Line shape analysis employing the DNMR5 program revealed an activation barrier for the **9** ⇌ **9′** rearrangement of $\Delta G^{\neq}_{inv}$ (268 K) = 14.9 ± 0.5 kcal mol^{-1}. This value is much smaller than was observed for the analogous dynamic process of the corresponding ansa-zirconocene complexes (see above). However, the respective reference value in the case of the hafnium containing complexes is considerably lower; the $\Delta G^{\neq}_{inv}$ value of the parent (s-*cis*-η^4-butadiene)$HfCp_2$ system is only 8.1 kcal mol^{-1} [12]. Thus introducing the particular ansa-metallocene backbone has increased the (s-*cis*-butadiene)metallocene inversion barrier by about 7 kcal mol^{-1}, an increase that is comparable with that observed upon going from (s-*cis*-η^4-butadiene)$ZrCp_2$ to the (s-*cis*-η^4-butadiene)ansa-zirconocene systems **8/8′**.

2.2. X-ray crystal structure analyses of the (s-*cis*-η^4-butadiene)metallocenes

The (s-*cis*-η^4-conjugated diene) Group 4 metallocene complexes exhibit a structural framework that is quite different from that of the late transition metal 1,3-diene complexes. These early transition metal systems feature a pronounced metallacyclopentene character; they are best described as of a σ^2,π structural type. Consequently, in a series of (2,3-dialkylbutadiene)$ZrCp_2$ and (2,3-arylbutadiene)$ZrCp_2$ complexes the Zr–C(1)/C(4) bonds are uniformely short (they are in a typical range of zirconium to carbon σ bonds) whereas the Zr–C(2)/C(3) distances are quite sensitive to the substitution pattern at carbon atoms C(2) and C(3) of the conjugated diene ligand [11,12]. Substituents that stabilize the C(2)–C(3) double bond in the σ^2,π-structured metallocene complex will lead to an increased Zr–C(2)/C(3) separation in the Zr(conjugated diene) envelope structure (Table 1).

For this reason we first had to determine the characteristic structural parameters of the parent compound (s-*cis*-η^4-butadiene)$ZrCp_2$ (**2a**) to serve as a reference that allowed us to judge whether a decreased D(1)–Zr–D(2) angle (as observed in the **6**-type complexes) leads to a noticeable structural change in the diene–metallo-

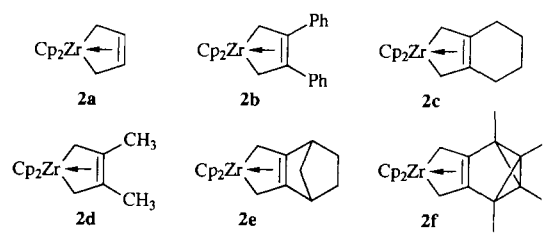

Form 2.

Table 2
Selected bond lengths (Å) and angles (°) for **2a**

Bond lengths			
Zr–C(1)	2.332(5)	Zr–C(4)	2.302(5)
Zr–C(2)	2.491(6)	Zr–C(3)	2.480(5)
Zr–C(10)	2.570(5)	Zr–C(15)	2.522(5)
Zr–C(11)	2.558(5)	Zr–C(16)	2.525(5)
Zr–C(12)	2.533(5)	Zr–C(17)	2.527(5)
Zr–C(13)	2.526(5)	Zr–C(18)	2.547(5)
Zr–C(14)	2.546(4)	Zr–C(19)	2.522(5)
Bond angles			
Zr–C(1)–C(2)	79.7(3)	Zr–C(4)–C(3)	79.8(3)
C(1)–C(2)–C(3)	129.6(6)	C(4)–C(3)–C(2)	128.1(6)
C(1)–Zr–C(4)	84.8(3)		

cene framework as is expected from an increased π character of the butadiene coordination to the early transition metal in this special ansa-metallocene environment — this is indeed observed:

Two η^5-cyclopentadienyls and a η^4-butadiene ligand are coordinated to the zirconium center in the bent metallocene complex **2a**. In the crystal the (s-*cis*-η^4-butadiene)zirconocene molecule deviates slightly from C_s symmetry. Therefore two slightly different distances between zirconium and the terminal butadiene carbon atoms are observed; both are just within the range expected of zirconium–carbon σ bonds (Zr–C(1), 2.332(5) Å; Zr–C(4), 2.302(5) Å), although both values are rather at the high end of that range [18]. The Zr–C(2) and Zr–C(3) distances are 2.491(6) and 2.480(5) Å respectively. Thus the (Zr–C(terminal))–(Zr–C(internal)) bond length difference of the Zr(butadiene) unit of **2a** is smaller than observed from all the other substituted (conjugated diene)$ZrCp_2$ complexes listed in Table 1. Consequently, the C(1)–C(2) (1.391(9) Å) and C(3)–C(4) (1.416(9) Å) bonds of **2a**

Table 3
Atomic coordinates and equivalent isotropic displacement parameters for **2a**, where U_{eq} is defined as one third of the trace of the orthogonalized U_{ij} tensor

	x ($\times 10^{-4}$)	y ($\times 10^{-4}$)	z ($\times 10^{-4}$)	U_{eq} ($\times 10^{-3}$ Å^2)
Zr	2473(1)	444(1)	6428(1)	23(1)
C(1)	1587(6)	−662(7)	4802(5)	55(2)
C(2)	1331(5)	−1871(8)	5604(6)	61(2)
C(3)	1039(4)	−1672(8)	6704(6)	55(1)
C(4)	895(4)	−153(8)	7308(7)	58(2)
C(10)	1490(5)	3159(6)	5805(5)	46(1)
C(11)	2406(5)	3058(6)	5157(5)	51(1)
C(12)	3307(5)	3236(6)	5917(5)	51(1)
C(13)	2938(4)	3426(6)	7007(5)	44(1)
C(14)	1833(4)	3379(6)	6943(4)	41(1)
C(15)	4472(4)	−133(9)	6611(7)	62(2)
C(16)	4170(5)	106(8)	7677(6)	60(2)
C(17)	3500(5)	−1172(9)	7980(6)	61(2)
C(18)	3408(5)	−2268(7)	7069(7)	66(2)
C(19)	3987(5)	−1620(10)	6176(6)	67(2)

are shorter than in the complexes **2b–2f**, although a long–short–long carbon–carbon bond length sequence is still maintained in **2a** (C(2)–C(3), 1.365(9) Å). The angle of fold of the ZrC_4H_6 envelope (i.e. the angle between the Zr, C(1), C(4) and C(1)–C(4) planes) in **2a** is 115.2°.

A view of the molecular geometry of the (s-*cis*-η^4-butadiene)zirconocene complex **2a** is given in Fig. 2; the selected bond lengths and angles of **2a** are listed in Table 2, and the atomic coordinates of **2a** in Table 3.

In the crystal, only one of the **8b**/**8b′** diastereoisomers is found, namely the diastereoisomer that has the butadiene C(2)–C(3) vector oriented toward the disubstituted Cp-ring system. As expected, the *n*-butyl group at the tetrahydroindenyl six-membered ring is arranged *trans* to the monosubstituted Cp substituent. A projection of the molecular structure of **8b** (with unsystematic atom numbering scheme) is shown in Fig. 3.

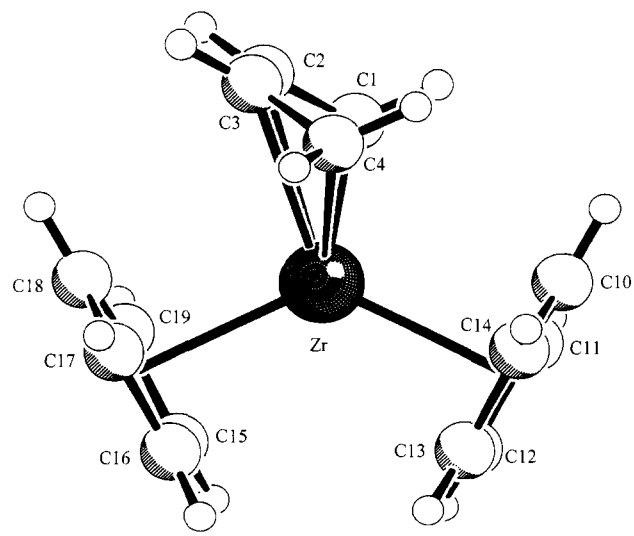

Fig. 2. A view of the molecular geometry of the (s-*cis*-η^4-butadiene)zirconocene complex **2a**.

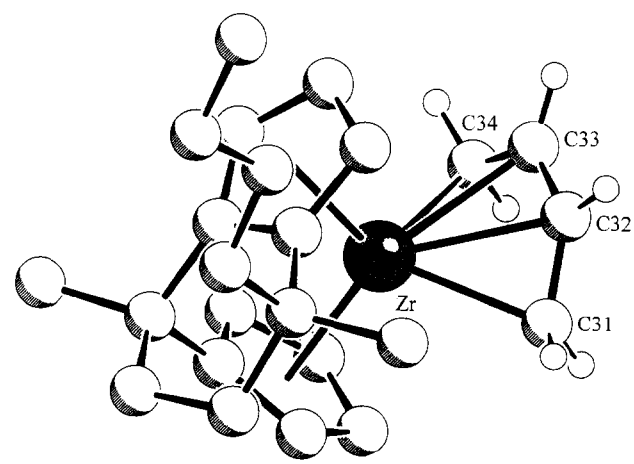

Fig. 3. A projection of the molecular structure of **8b** (with unsystematic atom numbering scheme).

The ansa-metallocene backbone in **8b** is much more rigid than in most other ansa-metallocene complexes. This is evident from the very small D(1)–Zr-D(2) angle of 114.7°, which to our knowledge is in fact the smallest D–M–D angle observed in a bent metallocene complex so far [7,13]. The effective opening angle of the bent metallocene is somewhat reduced, however, by a tilting distortion of the Cp rings towards the metal center. Thus the C(4)–C(9)–D(1) angle deviates by 15.1° from linearity. Similarly, this distortion at the monosubstituted Cp-ring systems measures 15.6° (i.e. C(4)–C(2)–D(2)). The resulting D(1)–Zr and D(2)–Zr distances are 2.22 and 2.23 Å respectively, which is only slightly smaller than observed in **2a** (see above; 2.26 and 2.24 Å).

The bonds between zirconium and the terminal butadiene carbon atoms are short (Zr–C(31), 2.324(12) Å; Zr–C(34), 2.301(13) Å). This is about the same metal–carbon bond length as in the reference compound **2a**. However, the bonds of the zirconium to the internal butadiene carbon atoms (Zr–C(32), 2.445(13) Å; Zr–C(33), 2.422(13) Å) are even shorter than in **2a**. The angle of fold (Zr–C(31)–C(34) vs. C(31)–C(34) planes] in **8b** is 109.6°. At the same time the difference between the C(31)–C(32) (1.38(2) Å) and C(34)–C(33) (1.40(2) Å) pair of bonds and the central C(32)–C(33) linkage (1.36(2) Å) is further decreased. There is still a slight long–short–long bond length sequence, but we notice a tendency toward a symmetrical butadiene coordination in the sequence **2b** → **2e** → **2a** → **8b**. It appears that the altered angle between the Cp planes of the ring-annulated C_1-bridged ansa-metallocene (as expressed by its extremely low value of the D(1)–Zr–D(2) angle) has helped much to advance another step towards a symmetrical π coordination in the (s-*cis*-η^4-conjugated diene) Group 4 metallocene series [19].

Selected bond lengths and angles of **8b** are given in Table 4, and the atomic coordinates of **8b** in Table 5. Details of the X-ray crystal structure analyses of complexes **2a** and **8b** are provided in Table 6 [19a].

Table 4
Selected bond lengths (Å) and angles (°) for **8b**

Bond lengths			
Zr–C(31)	2.324(12)	Zr–C(34)	2.301(13)
Zr–C(32)	2.445(13)	Zr–C(33)	2.422(13)
C(4)–C(5)	1.51(2)	C(4)–C(9)	1.53(2)
C(4)–C(10)	1.54(2)	C(4)–C(21)	1.54(2)
C(5)–C(6)	1.52(2)	C(6)–C(7)	1.55(2)
C(7)–C(8)	1.52(2)	C(7)–C(8)	1.52(2)
C(8)–C(9)	1.40(2)		
Bond angles			
Zr–C(31)–C(32)	78.0(8)	C(31)–Zr–C(34)	83.3(5)
Zr–C(34)–C(33)	77.6(8)	C(31)–C(32)–C(33)	126.7(14)
C5–C(4)–C(9)	109.0(10)	C(32)–C(33)–C(34)	129.3(14)
C5–C(4)–C(21)	113.7(11)	C(5)–C(4)–C(10)	108.5(11)
C(9)–C(4)–C(21)	101.1(9)	C(9)–C(4)–C(10)	112.9(11)
C(4)–C(5)–C(6)	116.5(11)	C(10)–C(4)–C(21)	111.7(10)
C(6)–C(7)–C(8)	108.1(11)	C(5)–C(6)–C(7)	115.6(11)
C(8)–C(9)–C(4)	122.2(10)	C(7)–C(8)–C(9)	123.3(10)

2.3. Extended Hückel theory calculations

The purpose of this theoretical study applying extended Hückel theory (EHT) [20a] and modified extended Hückel theory (MEHT) calculations [20b] is to trace the electronic effects of butadiene ring inversions in Cp_2Zr(butadiene) complexes with a narrow-angle biscyclopentadienyl geometry such as in **8** and **9** of the preceding work. Because of the general orbital situation of metallocenes [1,2], it is instructive to examine a Walsh diagram for the evolution of their frontier orbitals in dependence of the Cp_2M angle α. For the Cp_2Zr fragment this is represented in Fig. 4.

The most prominent changes occurring with the narrowing of α are seen for the $2a_1$ and b_1 orbitals, which increase and decrease respectively their energies. A perturbation molecular orbital analysis shows that these energy changes are primarily due to overlap changes in the respective Zr functions with the Cp ligands. In total the Cp rings show weaker interactions with the Zr center in the narrow-angle cases. This is expressed in the sum of total overlap populations between the Zr

Table 5
Atomic coordinates and equivalent isotropic displacement parameters for **8b** where U_{eq} is defined as one third of the trace of the orthogonalized U_{ij} tensor

	x (×10⁻⁴)	*y* (×10⁻⁴)	*z* (×10⁻⁴)	U_{eq} (×10⁻³ Å²)
Zr	6927(1)	1902(1)	1802(1)	29(1)
C(1)	7506(10)	4204(14)	1085(6)	37(3)
C(2)	8280(11)	4285(17)	1677(6)	42(3)
C(3)	8856(9)	2710(15)	1780(5)	36(3)
C(4)	8566(11)	−289(16)	1215(6)	41(3)
C(5)	8185(14)	−850(17)	529(6)	63(4)
C(6)	7120(15)	13(21)	126(7)	82(6)
C(7)	7125(10)	2018(19)	134(5)	47(3)
C(71)	7892(12)	2611(15)	−277(5)	44(3)
C(72)	8018(11)	4542(17)	−360(6)	47(3)
C(73)	8769(12)	4954(19)	−801(6)	58(4)
C(74)	8855(13)	6892(20)	−903(7)	66(4)
C(8)	7618(9)	2605(15)	810(5)	34(3)
C(9)	8454(9)	1677(14)	1249(5)	29(3)
C(10)	9788(11)	−925(17)	1490(7)	59(4)
C(11)	5919(11)	2722(27)	−138(7)	95(7)
C(21)	7768(10)	−885(14)	1618(6)	33(3)
C(22)	8051(10)	−664(14)	2281(6)	37(3)
C(23)	7050(11)	−862(14)	2482(6)	40(3)
C(24)	6179(12)	−1135(16)	1969(7)	52(4)
C(25)	6616(11)	−1129(15)	1431(6)	43(3)
C(31)	5001(11)	2520(17)	1460(8)	61(4)
C(32)	5444(12)	4079(19)	1721(8)	58(4)
C(33)	6211(13)	4316(18)	2289(8)	58(4)
C(34)	6743(11)	3089(20)	2736(6)	56(4)

Table 6
Details of the X-ray structure analyses of **2a** and **8b**

a (Å)	12.405(2)	12.182(2)
b (Å)	7.952(2)	7.748(1)
c (Å)	11.734(3)	21.831(6)
β (°)	92.55(2)	104.81(2)
V (Å^3)	1156.3(5)	1992.1(7)
Space group	$P2_1/c$ (No. 14)	$P2_1/c$ (No. 14)
Z	4	4
F(000) (e le chime)	560	864
μ (cm^{-1})	9.1	5.5
diffractometer	CAD4	CAD4
λ (Å)	0.71073	0.71073
θ_{max} (°)	26.3	22.5
data collected	2465	2755
data unique	2343	2610
data observed $\geqslant 2\sigma(I)$	2062	1698
refined parameters	136	229
$R(I \geqslant 2\sigma(I))$	0.046	0.060
$wR^2(I \geqslant 2\sigma(I))$	0.132	0.156
Goodness of fit	1.061	1.031

Programs used: SHELX-86, SHELX-93 and SCHAKAL-92.

center and the C_{Cp} atoms (e.g. overlap population $\Sigma(Zr-C_{Cp})_{124°} = 1.865$; $\Sigma(Zr-C_{Cp})_{110°} = 1.709$). In the narrow-angle region b_1 becomes of such low energy that it can now be considered to be part of the valence-type orbitals of a Cp_2Zr fragment. Such a narrow-angle fragment therefore possesses four instead of three frontier orbitals [1,2]. This is expected to have a noticeable influence on the orbital interactions with many types of moiety also with a butadiene ligand.

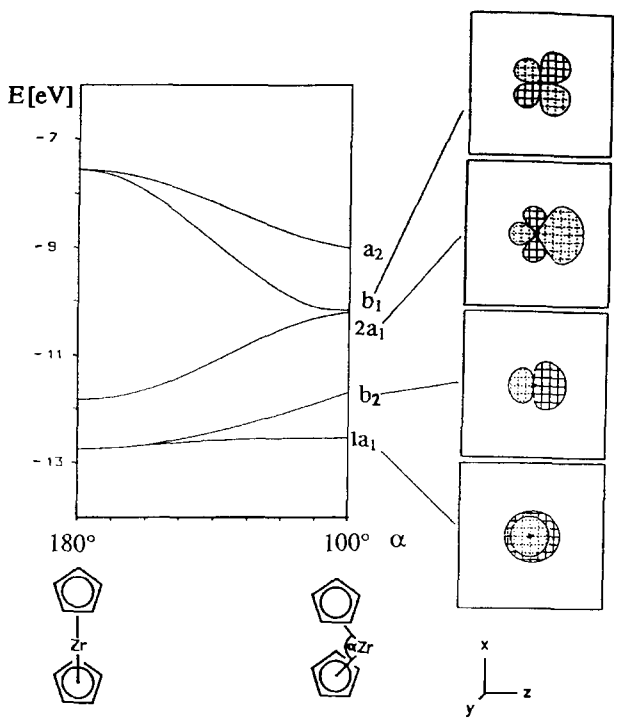

Fig. 4. Orbital correlation diagram of a Cp_2Zr fragment. Variation of the $Cp_{centroid}$–Zr–$Cp_{centroid}$ angle α.

The ring inversion processes were modelled by computing the conversion of the σ^2,π-Cp_2Zr(butadiene) structure **A**(α) [21] into the Cp_2Zr(butadiene) molecule **B**(α), which has a flat zirconapentene geometry and marks the transition state:

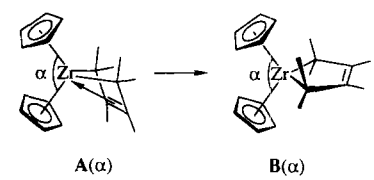

Form 3.

For these calculations the MEHT method [20b] was used. Two distinct situations have been chosen with $\alpha = 110°$ and 124°. **A**(124°) represents the geometry of the reference Cp_2Zr(butadiene) molecule, whose structure has been determined by an X-ray diffraction study (see above). The molecule with $\alpha = 110°$ is thought to mimic the narrow angle situation of molecules **8** and **9**. Multidimensional energy surfaces were therefore established for the interconversions of **A**(110°) and **A**(124°) and of **B**(110°) and **B**(124°). In these calculations the structures of the respective Cp_2Zr fragments, all C–H distances and the sp^2 geometry at the C_{int} atoms were kept fixed. The Zr–C, all C–C distances, the bond angles and the dihedral angles of the Zr-bound C atoms were allowed to relax.

In this way reaction paths for the **A**(α) $\rightleftharpoons$ **B**(α) processes were obtained, which led to the computed activation energies given in Table 7. In good agreement with the experimental data (12.6 kcal mol^{-1} for **2a** and 20.2 kcal mol^{-1} for **8a**/**8a'**) the narrow-angle molecule **A**(110°) shows a significantly higher inversion barrier than **A**(124°) given by the total energy difference of **B**(α)–**A**(α). A possible reason for this can be derived from the overlap populations of Table 7. An analysis of the sum of the total overlap populations for all (Zr–C)$_{butadiene}$ bonds first of all reveals stronger butadiene binding for **A**(110°) and **B**(110°), which apparently occurs at least to some extent on the expense of the Zr–Cp bond strength in these molecules (the narrow-angle Cp_2Zr fragments showed weaker Cp binding vide infra). The higher inversion barrier for the narrow-angle

Table 7
Calculated butadiene inversion and overlap population data of Cp_2Zr(butadiene) **2a**, the complexes **A**(α) and the transition states **B**(α)

α (°)	$\Delta E^{\dagger}_{calc}$ (kcal mol^{-1})	Total overlap population			
		C_{term} of **A**	C_{int} of **A**	C_{term} of **B**	C_{int} of **B**
124	10.9	0.428	0.078	0.618	−0.014
110	18.4	0.387	0.130	0.633	−0.011

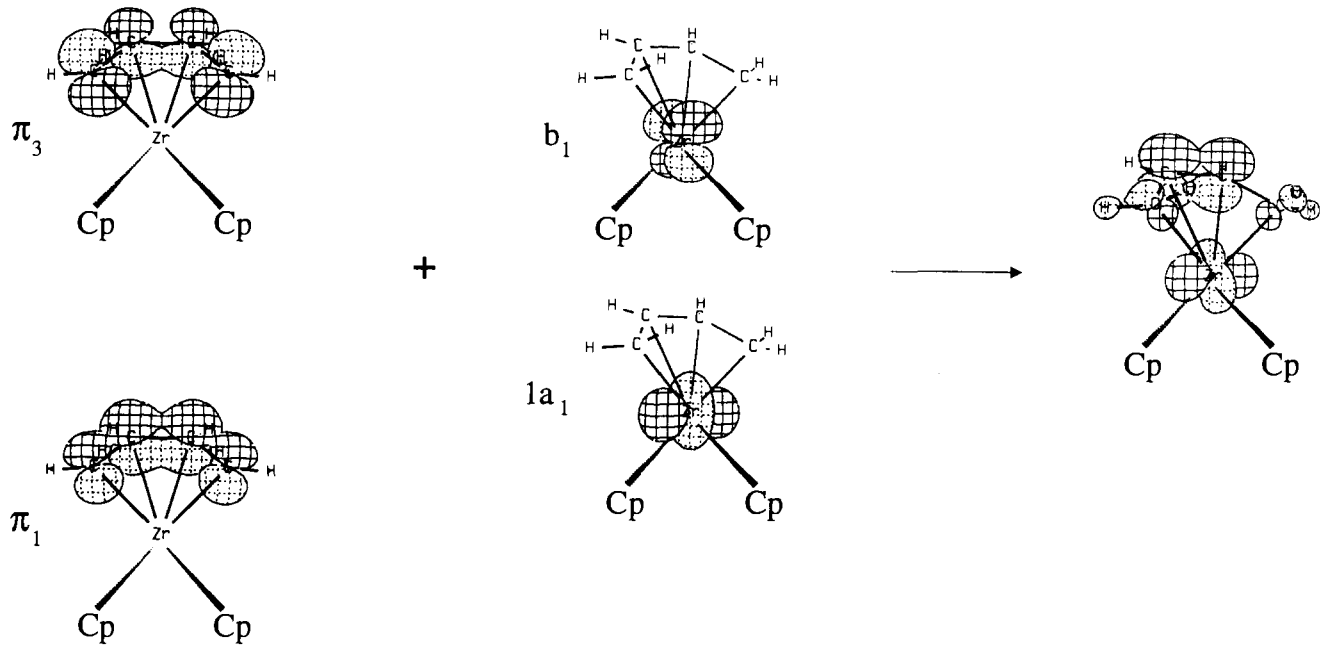

Fig. 5. Generalized CACAO orbital representation [1a] for the composition of the HOMO in A(α) molecules from the orbitals of a butadiene unit and a Cp_2Zr fragment.

molecule cannot, however, be directly related to this circumstance. The decisive fact in this respect is that the C_{int} atoms of the butadiene moiety are bound more strongly to the Zr center in A(110°) than in A(124°). Their release is more hindered in A(110°) when the molecules travel towards the transition states B(α).

An orbital analysis shows that the highest occupied molecular orbitals (HOMOs) of the A(α) species (Fig. 5) play a crucial role in the $Zr–C_{int}$ interactions.

In these HOMOs, π_1 and π_3 of the butadiene ligand are mixed together, so that the orbital coefficients at the C_{term} atoms decrease, while those at the C_{int} atoms increase, evolving the olefinic π bond of the $\sigma^2\pi$ bonded butadiene moiety. The Zr participation in the HOMO consists of $1a_1$ and b_1 contributions of the Cp_2Zr fragment, both of which orbital characters are in binding interaction to the C_{int} atoms. The zirconium b_1 orbital even points quite in the direction of the C_{int} lobes, thus reaching considerable overlap. In this manner the HOMOs of the A(α) molecules contribute to the binding between the Zr center and the C_{int} atoms (Fig. 5). Owing to the lower energy position of b_1 in the narrow-angle Cp_2Zr fragments the HOMO of A(110°) contains more b_1 orbital character, from which the stronger Zr–butadiene interaction then mainly results.

2.4. Conclusions

Opening of the bent metallocene wedge indeed leads to a marked change in the stereoelectronic properties of the central Group 4 transition metal center. In the six-membered ring annulated C_1-bridged ansa-metallocenes of the type discussed in this paper (**6–9**) the angle between the Cp planes is increased (and consequently the D(1)–M–D(2) angle decreased) by the steric requirements of the underlying fused hydrocarbon backbone. This results in a closing of the energy gap between the $2a_1$ and b_1 valence orbitals. The now substantially different spatial arrangement of orbitals available for bonding of added π ligands leads to markedly altered chemical characteristics of the Group 4 ansa-metallocene complexes having such a strained backbone. These specific changes in the electronic properties mean that the early transition metal center appears to behave as if it had moved slightly to the right in the periodic table. This slightly increased "late transition metal character" of zirconium or hafnium in these complexes can be nicely monitored by attaching the butadiene ligand. Structurally, the (s-*cis*-η^4-butadiene)zirconium complex (**8b**) has a noticeably increased π complex character compared with the reference structures of the parent bis(cyclopentadienyl)M systems. This description is strongly supported by the dynamic behavior of these complexes in solution. Both the C_1-bridged ansa-zirconocene and ansa-hafnocene butadiene systems have their "metallacyclopentene" inversion barrier increased by about 7–8 kcal mol^{-1}. This is a large effect that demonstrates how severely the electronic properties of the bent metallocene structure have been altered by changing the relative spatial arrangement of its Cp-ring systems. It is to be expected that reactions other than the butadiene metallocene

topomerization will prove similarly sensitive to the electronic changes brought about by changing the spatial arrangement of Cp-ring systems within the bent metallocene structures. This would then potentially provide an additional means of controlling the reactivity and selectivity patterns of stoichiometric reagents as well as catalyst systems derived from the Group 4 metallocenes.

3. Experimental section

3.1. General remarks

All reactions involving organometallic compounds were carried out in an inert atmosphere (argon) using Schlenk-type glassware or in a glove-box. All solvents were dried and distilled under argon prior to use. Instruments used for physical characterization of the products included a Bruker AC 200 P NMR spectrometer, a Bruker ARX 300 NMR spectrometer, a Varian Unity Plus 600 NMR spectrometer, and a Nicolet 5 DXC Fourier transform IR spectrometer. Melting points were obtained by differential scanning calorimetry (DuPont 910); elemental analyses were determined on a Foss–Heraeus CHN-Rapid elemental analyzer. The metallocene dihalides **6a**, **6b** and **7** were prepared as previously described [13]. The butadiene-magnesium reagent was prepared according to a literature procedure [9,15]. (Butadiene)zirconocene was prepared by the published method [11] and crystallized from toluene at −18 °C.

3.2. Preparation of (s-cis-η^4-butadiene)[(4-cyclopentadienylidene)-4,7,7-trimethyl-4,5,6,7-tetrahydroindenyl]zirconium (8a / 8a')

The dry reagents **6a** (0.90 g, 2.38 mmol) and (butadiene-magnesium). 2THF (0.62 g, 2.79 mmol) (THF = tetrahydrofuran) were mixed and cooled to −78 °C. 50 ml of a 1:1 mixture of ether:pentane was added dropwise with stirring. The mixture was allowed to warm to room temperature over night. A precipitate was removed by filtration and the clear red filtrate was kept at 0 °C for crystallization. The crystals of the (butadiene)zirconium complex **8a/8a'** were collected by filtration (yield, 0.85 g (96%); melting point (m.p.), 154 °C (decomposition); two diastereomers A and B in a 1:1.5 ratio). ^{1}H NMR (xylene-d_{10}, 600 MHz): δ 6.09 (B), 5.54 (B), 5.47 (B), 5.44 (A), 5.32 (A), 5.24 (A), 5.20 (A), 5.17 (B), 4.73 (B), 4.70 (A), 4.69 (A), 4.54 (B), 4.49 (A), 4.36 (B, m, each 1H, cyclopentadienyl CH), 4.85 (A + B, m, butadiene H_{meso}), 3.55, 3.43 (m, 1H each, B, butadiene H_{syn}), 3.40 (m, 2H, A, butadiene H_{syn}), 2.12, 2.06, 1.93, 1.52, 1.40 (m, indenyl CH_2 of A and B), 1.60, 1.00, 0.96 (s, each 3H, CH_3 of B), 1.57, 1.37, 1.18 (s, each 3H, CH_3 of A), −0.84, −1.07 (m, 1H each, B, butadiene H_{anti}), −0.89 (m, 2H, A, butadiene H_{anti}) ppm. ^{13}C NMR (benzene-d_6, 150.9 MHz, mixture of isomers): δ 131.3, 122.5, 117.1, 112.4, 105.9 (quart. C, Cp, one signal under solvent), 112.6, 112.3, 111.6, 110.5, 110.4, 110.3, 106.5, 104.2, 103.5, 101.8, 101.0, 99.9, 99.7, 99.5, 99.2, 93.7, 92.2, 87.8 (CH, Cp and butadiene), 53.8, 52.9, 51.4, 51.0 (CH_2, butadiene), 37.6, 37.3, 32.9, 32.6 (CH_2, indenyl), 36.1, 36.0, 31.8, 31.1 (quart. C, indenyl C(4), C(7)), 34.6, 34.4, 29.9, 28.5, 27.9, 27.6 (CH_3) ppm. IR (KBr): $\tilde{\nu}$ 3092, 2958, 2916, 1495, 1452, 1099, 1072, 1046, 1024, 860, 851, 812, 790, 770, 740, 731 cm^{-1}. Anal. Found: C, 67.44; H, 7.06. $C_{21}H_{26}Zr$ (M = 369.7) Calc.: C, 68.23; H, 7.09%.

3.3. Preparation of (s-cis-η^4-butadiene)[7-n-butyl-(4-cyclopentadienylidene)-4,7-dimethyl-4,5,6,7-tetrahydroindenyl]zirconium (8b / 8b')

Analogous to the above-described treatment, 1.0 g (2.33 mmol) of **6b** with 0.62 g (2.80 mmol) of (butadiene-magnesium). 2THF gave 0.9 g (94%) of a mixture of **8b/8b'** in a 1:1.5 diastereoisomer ratio (m.p. 202 °C). The crystals obtained from ether:pentane (1:1) were suitable for the X-ray crystal structure analysis (see Table 6 for details). ^{1}H NMR (xylene-d_{10}; 600 MHz, mixture of both isomers A and B): δ 6.13, 5.54, 5.48, 5.35, 5.25, 5.21 (double intensity), 4.75, 4.72, 4.70, 4.55, 4.47, 4.36 (m, 1H each, cyclopentadienyl of A + B, 1H under C_4H_6 multiplet), 5.9 (br.m, butadiene H_{meso}, A + B), 3.56 and 3.39 (m, 1H each, butadiene H_{syn} of the major isomer B), 3.43 (m, 2H, butadiene H_{syn} of A), 2.1–1.9, 1.7–1.4 (several m, indenyl CH_2), 1.40–1.05 (several m, *n*-butyl CH_2), 0.88 (m, *n*-butyl–CH_3 of A), 0.82 (m, *n*-butyl–CH_3 of B), 1.61 and 0.95 (s, each 1H, CH_3 of B), 1.58 and 1.33 (s, each 3H, CH_3 of A), −0.81 and −1.05 (m, each 1H, butadiene H_{anti} of B), −0.89 (m, 2H, butadiene H_{anti} of A) ppm. Anal. Found: C, 68.98; H, 8.04. $C_{24}H_{32}Zr$ (M = 411.7) Calc.: C, 70.01; H, 7.83%.

3.4. Reaction of [(4-cyclopentadienylidene)-4,7,7-trimethyl-4,5,6,7-tetrahydroindenyl]hafnium dichloride with "butadiene-magnesium"

The ansa-metallocene dichloride **7** (0.31 g, 0.66 mmol) was mixed with 0.22 g (0.99 mmol) of the butadiene-magnesium reagent. At −78 °C, pre-cooled toluene (40 ml) was added dropwise with stirring. The mixture was warmed to ambient temperature and stirred for 18 h. A precipitate was removed by filtration and the solvent removed from the clear filtrate in vacuo to give 300 mg (99%) of the **9/9'** mixture (1:1.5) (m.p., 134 °C). ^{1}H NMR (toluene-d_8; 600 MHz, 223 K, several signals of the isomers A and B are overlapping): δ 5.87, 5.51, 5.28, 5.24, 5.10, 5.01 (double intensity),

Table 8
Parameters used in the EHT [20a] and MEHT [20b] calculations

Element	Orbital	H_{ii} (eV)	ξ_1	ξ_2	C^1	C^2
H	1s	−13.6	1.30			
C	2s	−21.4	1.625			
	2p	−11.4	1.625			
Zr	4d	−12.1	3.835	1.505	0.6211	0.5796
	5s	−10.1	1.776			
	5p	−6.86	1.817			

Table 9
MEHT optimized bond distances of the zirconapentene moiety in **A**(110°) **A**(124°), **B**(110°) and **B**(124°)

	$Zr-C_{term}$ (Å)	$Zr-C_{int}$ (Å)	$C_{term}-C_{int}$ (Å)	$C_{int}-C_{int}$ (Å)
A(110°)	2.26	2.42	1.60	1.51
A(124°)	2.23	2.57	1.61	1.51
B(110°)	2.11	2.96	1.75	1.48
B(124°)	2.13	3.00	1.74	1.48

4.91, 4.67 (double intensity), 4.63, 4.40, 4.37, 4.31 (m, cyclopentadienyl), 5.0–4.9 (m, 2H, butadiene H_{meso}), 3.41 and 3.24 (m, each 1H, butadiene H_{syn} of the major isomer B), 3.32 (m, 2H, butadiene H_{syn} of A), 2.1–1.2 (several m, indenyl CH_2), 1.47, 0.94, 0.92 (s, each 3H, CH_3 of B), 1.44, 1.31, 1.14 (s, each 3H, CH_3 of A), −1.07 and −1.19 (m, 2H, butadiene H_{anti} of B), −1.06 (m, 2H, butadiene H_{anti} of A) ppm.

3.5. Extended Hückel calculations

The parameters used in the EHT [20a] and MEHT [20b] calculation were taken from earlier work [21] and are given in Table 8.

The calculations of the butadiene inversions were performed with fixed Cp_2Zr structural backbones. The $(C-C)_{Cp}$, $(C-H)_{Cp}$ and the $(Zr-Cp)_{centroid}$ distances were 1.45 Å, 1.04 Å and 2.02 Å respectively. Within the zirconapentene unit the C_{int} sp^2 geometry and all C–H bond lengths (1.03 Å) were kept fixed. All other geometrical degrees of freedom such as the Zr–C, $C_{term}-C_{int}$, $C_{int}-C_{int}$ bond lengths and the bond and dihedral angles at C_{term} were optimized at each point of the energy surfaces.

Optimized bond distances of **A**(110°), **A**(124°), **B**(110°) and **B**(124°) are given in Table 9.

Acknowledgments

Financial support from the Fonds der Chemischen Industrie, the Alfried Krupp von Bohlen und Halbach-Stiftung, the Swiss National Science Foundation and the EC (COST program) is gratefully acknowledged.

References and notes

[1] H.H. Brintzinger and L.S. Bartell, *J. Am. Chem. Soc., 92* (1970) 1105.

[2] J.W. Lauher and R. Hoffmann, *J. Am. Chem. Soc., 98* (1976) 1729.

[3] (a) W. Kaminsky, K. Külper, H.H. Brintzinger and F.R.W.P. Wild, *Angew. Chem., 97* (1985) 507; *Angew. Chem., Int. Edn. Engl., 24* (1985) 507; J.A. Ewen *J. Am. Chem. Soc., 106* (1984) 6355. For a review of the early work in this field see H. Sinn and W. Kaminsky, *Adv. Organomet. Chem., 18* (1980) 99, and references cited therein.
(b) G.G. Hlatky, H.W. Turner and R.R. Eckman, *J. Am. Chem. Soc., 111* (1989) 2728; X. Yang, C.L. Stern and T.J. Marks, *J. Am. Chem. Soc., 113* (1991) 3623; *Angew. Chem., 104* (1992) 1406; *Angew. Chem., Int. Edn. Engl., 31* (1992) 1375; C. Pellecchia, A. Immirzi, A. Grassi and A. Zambelli, *Organometallics, 12* (1993) 4473; M. Bochmann, S.J. Lancaster, M.B. Hursthouse and K.M. Abdul Malik, *Organometallics, 13* (1994) 2235. Reviews have been given by R.F. Jordan, *Adv. Organomet. Chem., 32* (1991) 325; M. Bochmann, *Angew. Chem., 104* (1992) 1206; *Angew. Chem., Int. Edn. Engl., 31* (1992) 1181.

[4] See for example H. Schnutenhaus and H.H. Brintzinger, *Angew. Chem., 91* (1979) 837; *Angew. Chem., Int. Edn. Engl., 18* (1979) 777; J.A. Smith, J. von Seyerl, G. Huttner and H.H. Brintzinger, *J. Organomet. Chem., 173* (1979) 175; W. Röll, L. Zsolnai, G. Huttner and H.H. Brintzinger, *J. Organomet. Chem., 322* (1987) 65; J.A. Ewen, L. Haspeslagh, J.L. Atwood and H. Zhang, *J. Am. Chem. Soc., 109* (1987) 6544; C.M. Fendrick, L.D. Schertz, V.W. Day and T.J. Marks, *Organometallics, 7* (1988) 1828; W.A. Herrmann, J. Rohrmann, E. Herdtweck, W. Spaleck and A. Winter, *Angew. Chem., 101* (1989) 1536; *Angew. Chem., Int. Edn. Engl., 28* (1989) 1511; D.T. Mallin, M.D. Rausch, Y.-G. Lin, S. Dong and J.C.W. Chien, *J. Am. Chem. Soc., 112* (1990) 2030; S. Collins, Y. Hong, R. Ramanchandran and N.J. Taylor, *Organometallics, 10* (1991) 2349; J.A. Bandy, M.L.H. Green, I.M. Gardiner and K. Prout, *J. Chem. Soc., Dalton Trans.*, (1991) 2207; T.K. Hollis, A.L. Rheingold, N.P. Robinson, J. Whelan and B. Bosnich, *Organometallics, 11* (1992) 2812; M.E. Huttenloch, J. Diebold, U. Rief, H.-H. Brintzinger, A.M. Gilbert and T.J. Katz, *Organometallics, 11* (1992) 3600; P. Burger, J. Diebold, S. Gutmann, H.-U. Hund and H.H. Brintzinger, *Organometallics, 11* (1992) 1319; B. Dorer, J. Diebold, O. Weyand and H.H. Brintzinger, *J. Organomet. Chem., 427* (1992) 245; G.H. Llinas, S.-H. Dong, D.T. Mallin, M.D. Rausch, Y.-G. Lin, H.H. Winter and J.C.W. Chien, *Macromolecules, 25* (1992) 1242; R. Gomez, T. Cuenca, P. Royo and E. Hovestreydt, *Organometallics, 10* (1991) 2516; G. Erker, S. Wilker, C. Krüger and R. Goddard, *J. Am. Chem. Soc., 114* (1992) 10983; G. Erker, S. Wilker, C. Krüger and M. Nolte, *Organometallics, 12* (1993) 2140, and literature cited in these references.

[5] J.A. Ewen, R.L. Jones, A. Razawi and J.D. Ferrara, *J. Am. Chem. Soc., 110* (1988) 6255; W. Spaleck, M. Antberg, J. Rohrmann, A. Winter, B. Bachmann, P. Kiprof, J. Behm and W.A. Herrmann, *Angew. Chem., 104* (1992) 1373; *Angew. Chem., Int. Edn. Engl., 31* (1992) 1347.

[6] For a review of recent industrial application see M. Aulbach and F. Küber, *Chem. Unserer Zeit, 28* (1994) 197.

[7] For a compilation of many of such structural reference data see U. Höweler, R. Mohr, M. Knickmeier and G. Erker, *Organometallics, 13* (1994) 2380.

[8] G. Erker, J. Wicher, K. Engel, F. Rosenfeldt, W. Dietrich and C. Krüger, *J. Am. Chem. Soc., 102* (1980) 6344; G. Erker, J. Wicher, K. Engel and C. Krüger, *Chem. Ber., 115* (1982)

3300; U. Dorf, K. Engel and G. Erker, *Organometallics, 2* (1983) 462; P. Czisch, G. Erker, H.-G. Korth and R. Sustmann, *Organometallics, 3* (1984) 945.

[9] H. Yasuda, Y. Kajihara, K. Mashima, K. Nagasuna, K. Lee and A. Nakamura, *Organometallics, 1* (1982) 388; Y. Kai, N. Kanehisa, K. Miki, N. Kasai, K. Mashima, K. Nagasuna, H. Yasuda and A. Nakamura, *J. Chem. Soc., Chem. Commun.*, (1982) 191.

[10] Meanwhile, a variety of stable s-*trans*-η^4-diene complexes have been found using other metal complex fragments of similar electronic characteristics. See for example A.D. Hunter, P. Legzdins, C.R. Nurse, F.W.B. Einstein and A.C. Willis, *J. Am. Chem. Soc., 107* (1985) 1791; A.D. Hunter, P. Legzdins, F.W.B. Einstein, A.C. Willis, B.E. Bursten and M.G. Gatter, *J. Am. Chem. Soc., 108* (1986) 3843; H. Yasuda and A. Nakamura, *Angew. Chem., 99* (1987) 745, *Angew. Chem., Int. Edn. Engl., 26* (1987) 723; T. Okamoto, H. Yasuda, A. Nakamura, Y. Kai, N. Kanehisa and N. Kasai, *J. Am. Chem. Soc., 110* (1988) 5008; E. Melendez, A.M. Arif, A.L. Rheingold and R.D. Ernst, *J. Am. Chem. Soc., 110* (1988) 8703; N.J. Christensen, A.D. Hunter and P. Legzdins, *Organometallics, 8* (1989) 930; S.A. Benyunes, M. Green and M.J. Grimshire, *Organometallics, 8* (1989) 2268; S.A. Benyunes, M. Green, M. McPartlin and C.B.M. Nation, *J. Chem. Soc., Chem. Commun.*, (1989) 1887; S.A. Benyunes, J.P. Day, M. Green, A.W. Al-Saadoon and T.L. Waring, *Angew. Chem., 102* (1990) 1505; *Angew. Chem., Int. Edn. Engl., 29* (1990) 1416; V.-J. Vong, S.-M. Peng and R.-S. Liu, *Organometallics, 9* (1990) 2187; N.J. Christensen, P. Legzdins, F.W.B. Einstein and R.H. Jones, *Organometallics, 10* (1991) 3070; N.J. Christensen, P. Legzdins, J. Trotter and V.C. Yee, *Organometallics, 10* (1991) 4021; R.D. Ernst, E. Melendez, L. Stahl and M.L. Ziegler, *Organometallics, 10* (1991) 3635; G.E. Herberich, U. Englert, K. Linn, P. Roos and J. Runsink, *J. Chem. Ber., 124* (1991) 975; W.-J. Vong, S.-M. Peng, S.-H. Lin, W.-J. Lin and R.-S. Liu, *J. Am. Chem. Soc., 113* (1991) 573; M.-H. Cheng, Y.-H. Ho, S.-L. Wang, C.-Y. Cheng, S.-M. Peng, G.-H. Lee and R.-S. Liu, *J. Chem. Soc., Chem. Commun.*, (1992) 45; J.D. Debad, P. Legzdins, M.A. Young, R.J. Batchelor and F.W.B. Einstein, *J. Am. Chem. Soc., 115* (1993) 2051.

[11] G. Erker, K. Engel, C. Krüger and A.-P. Chiang, *Chem. Ber., 115* (1982) 3311; G. Erker, K. Engel, C. Krüger and G. Müller, *Organometallics, 3* (1984) 128; C. Krüger, G. Müller, G. Erker, U. Dorf and K. Engel, *Organometallics, 3* (1985) 215.

[12] G. Erker, C. Krüger and G. Müller, *Adv. Organomet. Chem., 24* (1985) 1.

[13] G. Erker, C. Psiorz, C. Krüger and M. Nolte, *Chem. Ber., 127* (1994) 1551; C. Psiorz, G. Erker, R. Fröhlich and M. Grehl, *Chem. Ber., 128* (1995) 357; G. Erker, C. Psiorz, M. Grehl, C. Krüger, R. Noe and M. Nolte, *Tetrahedron, 51* (1995) 4347; G. Erker, C. Psiorz and R. Fröhlich, *Z. Naturforsch., 506* (1995) 469.

[14] M.S. Erickson, J.M. Cronan, J.G. Garcia and M.L. McLaughlin, *J. Org. Chem., 57* (1992) 2504. For related coupling reactions involving fulvenes see for example K. Hafner, *Angew. Chem., 70* (1958) 419; M. Neuenschwander, P. Kronig, S. Schönholzer, M. Slongo, B. Uebersax and C. Rentsch, *Croat. Chem. Acta, 53* (1980) 625; P. Kronig, M. Slongo and M. Neuenschwander, *Makromol. Chem., 163* (1982) 359.

[15] K. Fujita, Y. Ohnuma, H. Yasuda and H. Tani, *J. Organomet. Chem., 113* (1976) 201.

[16] D.S. Stephenson and G. Binsch, *QCPE, 10* (1978) 365; G. Binsch, *Dyn. Nucl. Magn. Reson. Spectrosc.*, (1975) 45; G. Binsch and H. Kessler, *Angew. Chem., 92* (1980) 445; *Angew. Chem., Int. Edn. Engl., 19* (1980) 411.

[17] M.L.H. Green, L.-L. Wong and A. Sella, *Organometallics, 11* (1992) 2660, and references cited therein.

[18] For reference values see A.G. Orpen, L. Brammer, F.H. Allen, O. Kennard and D.G. Watson, *J. Chem. Soc., Dalton Trans.*, (1989) S1.

[19] A similar effect is observed when the f-element thorium is introduced instead of the d-metal zirconium; see G. Erker, T. Mühlenbernd, R. Benn and A. Rufínska, *Organometallics, 5* (1986) 402; G.M. Smith, H. Suzuki, D.C. Sonnenberger, V.W. Day and T.J. Marks, *Organometallics, 5* (1986) 549.

[19a] Further details of the X-ray structure determinations may be obtained from the Fachinformationszentrum Karlsruhe, Gesellschaft für wissenschaftlich-technische Information mbH, D-76344 Eggenstein-Leopoldshafen, Germany. Requests should contain the deposition number CSD-58827, names of authors, and citation of this article.

[20] (a) C. Mealli, D.M. Proserpio, *J. Chem. Educ., 67* (1990) 399. (b) A.B. Anderson, *J. Chem. Phys., 62* (1975) 1187; D.A. Pensak and R.J. McKinney, *Inorg. Chem., 18* (1979) 3407.

[21] K. Tatsumi, H. Yasuda and A. Nakamura, *Isr. J. Chem., 23* (1983) 145.